Persistent Radicals and Transfer Reactions in the Postpolymerization of Methyl Methacrylate

Nuria García,*,† Pilar Tiemblo,† Laura Hermosilla,‡ Paloma Calle,‡ Carlos Sieiro,‡ and Julio Guzmán†

Instituto de Ciencia y Tecnología de Polímeros, C.S.I.C., Juan de la Cierva 3, 28006 Madrid, Spain, and Departamento de Química Física Aplicada, Universidad Autónoma de Madrid, 28049 Madrid, Spain

Received April 18, 2007; Revised Manuscript Received August 10, 2007

ABSTRACT: The posteffects in the polymerization of methyl methacrylate at low monomer conversions are studied. The experimental two-step method consists of a short initial photoinduced polymerization period and subsequent register of the monomer concentration evolution in the dark. After switching off the light, the radical concentration drops sharply, but a nonnegligible concentration of persistent radicals continues the polymerization reaction for long periods of time, yielding ultrahigh molecular weight materials (over 10 000 monomer units). By a fitting procedure applied to the conversion−time curves obtained during the dark period, average values of the termination rate coefficients, $\langle k_t \rangle$, scarcely exceeding 10 000 L mol^{-1} s^{-1}, and radical concentrations at the beginning of the postpolymerization about 10^{-8} mol L^{-1} are determined. The reliability of these fitting results is checked by the design of reactions with similar polymerization rate but under steady-state conditions. The molecular weight of the polymers synthesized during the dark period is controlled by the transfer reactions to the monomer and to the initiator. Both transfer reaction constants are estimated by using a method based on the analysis of the instantaneous chain length distribution. The extremely low $\langle k_t \rangle$ values obtained by the analysis suggest that the power-law exponents which describe the chain-length dependency of k_t should be higher than the unity for long radicals even in dilute solution (i.e., at low monomer conversions).

Introduction

The research on free-radical polymerization kinetics is a fashionable field since new challenges and questions have risen with the advent of modern and sophisticated synthetic and analytical techniques. The relevance of free-radical polymerization reactions in industry makes this topic attractive not only from the academic but also from the technical and practical points of view. The complexity of the study of these systems lies in the wide diversity of coexistent species with different reactivities and chain lengths. This implies serious problems in the determination of absolute values of the rate coefficients that control the process. In this sense, the efforts made by the IUPAC Working Party on Polymerization Kinetics and Processes to provide reliable values of the rate parameters for free-radical polymerizations are remarkable. After the publication of a paper series dealing with benchmark values of propagation rate coefficients, k_p, for different monomers,[1] the ultimate aim of this IUPAC task group is the termination reaction.[2,3] The termination between radicals is a diffusion-controlled event; this means that the termination rate coefficient, k_t, depends not only on the chain length of the involved radicals but also on the viscous properties of the surroundings. Theoretical and experimental approaches to the study of the chain-length and conversion dependency of k_t have for decades caught the attention of many researchers, the vast literature on this topic being a proof.[4−17]

The value usually obtained in most of the experimental works described in the literature is an overall or average rate coefficient for termination, $\langle k_t \rangle$, defined as[2]

$$\langle k_t \rangle = \sum_{\text{all } i} \sum_{\text{all } j} k_t^{ij} \frac{[R_i][R_j]}{[R]^2} \quad (1)$$

where k_t^{ij} is the termination rate coefficient between radicals of chain length i and j, of concentration $[R_i]$ and $[R_j]$, respectively, over the total radical concentration [R]. From steady-state experiments varying the reaction conditions and the polymerization time, the dependency of $\langle k_t \rangle$ on the viscosity of the medium, on the monomer nature, and on the conversion can be determined. However, given that under those conditions radicals of many different chain lengths are simultaneously present, the inference of k_t^{ij} is experimentally unattainable.

To tackle this question, a different experimental approach has been developed that consists of the determination of termination rate coefficients between radicals of identical chain lengths, k_t^{ii}. In this regard, the so-called single-pulse pulsed-laser polymerization technique, SP-PLP, pioneered by Buback et al.[18] is probably the most widely known one. This technique is based on the application of a laser pulse to a polymerizable system and subsequently on-line registration of the monomer conversion. The assumption is made that the short width of the laser pulse makes the coexistent radicals be of almost identical chain length during the time after the pulse. The main shortcomings arise from an accurate register of monomer conversion and from the need to accumulate signals to obtain reliable results for some systems. A recent improvement on this technique consists of the monitoring of the radical concentration decay by time-resolved electron paramagnetic resonance (EPR), which provides a greater accuracy than the monomer concentration register and turns into easier data analysis.[19] Maybe, the only objection to this technique is that radical concentrations not exceeding 10^{-7} mol L^{-1} are almost undetectable by EPR but by no means can be considered negligible in the analysis.

* Corresponding author. E-mail: ngarcia@ictp.csic.es.
† C.S.I.C.
‡ Universidad Autónoma de Madrid.

10.1021/ma070908a CCC: $37.00
Published on Web 10/12/2007

From these SP-PLP experiments, the values of k_t^{ii} and not k_t^{ij} are made available. A work by de Kock et al.[20] described a simple modification to the SP-PLP technique to gain access to k_t^{ij}. This is based on the application of a second pulse laser shortly after the first one; knowing the radical concentrations originated from both laser pulses, the k_t^{ij} values would be directly calculated. However, the experimental limitations imposed by the calculus still make this method inaccurate for long chain radicals.

Very recently, Barner-Kowollik and co-workers have proved that k_t^{ii} values can also be accessible by reversible addition−fragmentation chain transfer (RAFT) in combination with measurements of polymerization rate.[21] They anticipated the potential determination of k_t^{ij} values by using this experimental approach.[22]

The experimental k_t^{ii} values determined as above-described agree fairly well with the so-called "composite model" states by Smith et al.[17] This model assumes the usual power-law dependency of k_t^{ii} on chain length i

$$k_t^{ii} = k_t^{1,1} i^{-\beta} \tag{2}$$

where $k_t^{1,1}$ is the termination rate coefficient for two monomeric free radicals and β is the exponent which assesses the chain-length dependency, in such a way that the higher its value, the stronger the decline of k_t^{ii} with increasing radical length. The "composite model" proposes $\beta \approx 0.5$ for small radicals and a smoother chain-length dependency for long radicals ($i > 100$) holding $\beta \approx 0.16$. The model is not only consistent with the available experimental k_t^{ii} values but also enables an interpretation of $\langle k_t \rangle$ values obtained under steady-state conditions.

In a recent paper,[23] we obtained $\langle k_t \rangle$ values barely exceeding 10^4 L mol^{-1} s^{-1} during the postpolymerization of different methacrylic monomers. These $\langle k_t \rangle$ values can hardly be explained by chain-dependent k_t models which assume power-law exponents lower than the unity. Such $\langle k_t \rangle$ values could be considered as reasonable during the classical posteffect experiments, i.e., at relative high monomer conversion and where viscosity effects on the radical diffusion are expected.[12] On the contrary, the peculiarity of our postpolymerization experiments was that we detected the presence of long-lived radicals at very low monomer conversions and in systems where the rate of initiation was null. Under these conditions, the preferential stop-chain event was the transfer to the monomer; notwithstanding this fact, ultrahigh molecular weight polymers were obtained. These experiments were carried out with three methacrylic monomers bearing bulky ester residue, which, in principle, leads to expect lower $\langle k_t \rangle$ values.[24]

The aim of the present work is to investigate this posteffect on the most widely studied methacrylic monomer, methyl methacrylate (MMA). The same experimental protocol which was previously used will be followed to analyze the polymerization kinetics of MMA but extending the study to different initiators and reaction conditions. These unusual conditions enable the determination of $\langle k_t \rangle$ and the transfer rate constants to the monomer and to the initiators, which definitively contributes to obtain a better knowledge of the free-radical polymerization kinetics in general and of MMA reactions, in particular.

Experimental Section

Materials. Methyl methacrylate (MMA, Fluka, 99%) was distilled under high vacuum before use. The photoinitiators, 2,2-dimethoxy-2-phenylacetophenone (DMPA, Aldrich, 99%) and 2-methyl-4′-(methylthio)-2-morpholinopropiophenone (MMPA, Aldrich, 98%), were used as received. Azobis(isobutyronitrile) (AIBN, Fluka, 98%) was purified by recrystallization from methanol.

Polymerization Reactions. *Photopolymerizations and Reactions in the Dark.* MMA solutions (5 mL) with different DMPA and MMPA concentrations ranging from 0.1 mol L^{-1} (0.128 g of DMPA or 0.139 g of MMMP) to 8×10^{-3} mol L^{-1} (1.0×10^{-2} g of DMPA or 1.1×10^{-2} g of MMMP) were prepared. The solutions were subjected to several freeze−pump out−thaw to remove dissolved oxygen. 0.8 mL of the degassed solution was placed inside a jacketed cylindrical quartz cell (path length 5 mm), which was connected to a thermostatic bath with recirculating water at 25 °C. The photopolymerization reaction was performed inside an ultraviolet cross-linker (UPV, model CL-1000L) operating at $\lambda = 365$ nm. The exposure times ranged between 2 and 25 min, depending on the initiator type and concentration and the desired conversion. Thus, 3 min of exposure time with a DMPA concentration of 3×10^{-2} mol L^{-1} was needed to reach a 5% conversion of monomer into polymer, whereas 5 min was needed to reach the same conversion when MMMP was used as initiator at the same concentration. The monomer concentration was monitored by FT-IR spectroscopy (Spectrum One, Perkin-Elmer) in the region of the first overtone of C−H stretching vibrations, at around 6170 cm^{-1}. The first spectrum after UV light exposure, which gave the initial monomer conversion, was recorded in all the reactions 1 min after the illumination period. The sample was kept inside the IR cavity during the dark period, and the monomer concentration was sequentially registered. After a certain conversion was reached, the resulting polymer was precipitated in methanol containing traces of hydroquinone to prevent further polymerization and was isolated prior to SEC analysis.

Blank experiments, reproducing the reaction conditions but without previous photopolymerization, were carried out to check whether primary radicals from the photoinitiators could be generated during the dark time.

An additional polymerization reaction initiated by a pulsed laser (Quanta-Ray Nd/YAG laser, Spectra Physics, operating at 355 nm, 50 mJ per pulse, 0.1 s between laser pulses) was carried out. The initiator was MMMP at a concentration of 2×10^{-2} mol L^{-1}. The pulsed laser polymerization reaction took place inside a quartz cell identical to that above-described, and 1800 pulses were needed to reach 3% conversion. After laser pulsing, the subsequent polymerization in the dark was also monitored by FT-IR spectroscopy.

Thermal Polymerizations. The thermal polymerizations of MMA at 25 °C were carried out with AIBN acting as initiator. The AIBN concentrations were varied from 1×10^{-2} to 0.45 mol L^{-1} (from 8.2×10^{-3} to 0.37 g of AIBN in 5 mL). The reaction protocol to perform the thermal polymerization was identical to that used for the photopolymerizations, also in regard to the first photoinduced polymerization period inside the ultraviolet cross-linker.

Size Exclusion Chromatography Analysis. Molecular weight distributions (MWD) were determined by means of size-exclusion chromatography (SEC) using a Waters 1515 HPLC pump, a Waters 2414 refractive index detector, and a set of three Waters columns with nominal pore sizes of 10^2, 10^4, and 10^6 Å. The eluent was tetrahydrofuran at 35 °C pumped at 1 mL min^{-1}. The SEC setup was calibrated against polystyrene (PS) standards of narrow polydispersity (MW = 580−5×10^6 g mol^{-1}, Polymer Standards). Absolute molecular weights of the pMMA samples were estimated via the principle of universal calibration[25] using the Mark−Houwink parameters $K = 1.14 \times 10^{-4}$ dL g^{-1}, $\alpha = 0.716$ for PS and $K = 9.44 \times 10^{-5}$ dL g^{-1}, $\alpha = 0.719$ for pMMA were taken from the literature.[26,27]

Results and Discussion

Photopolymerization of Methyl Methacrylate. Previous to the analysis of the reaction kinetics in the dark, an estimation of the radical concentration during the photoinitiated polymerization period, $[R]_{ph}$, can be done. According to eq 3, where $[M]_{0,ph}$ and $[M]_{ph}$ are the initial and instantaneous monomer

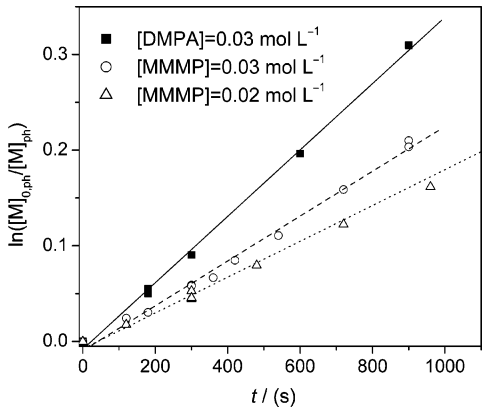

Figure 1. Conversion−time curves in 2,2-dimethoxy-2-phenylacetophenone (DMPA)-initiated and 2-methyl-4′-(methylthio)-2-morpholinopropiophenone (MMMP)-initiated bulk free-radical photopolymerization of methyl methacrylate at 25 °C. The photoinitiator type and concentrations are given within the figure. Straight lines represent the linear fits of the data.

concentrations, the plots of monomer conversion as a function of irradiation time would yield straight lines if the photoinduced polymerizations proceeded under steady-state conditions.

$$\ln\left(\frac{[M]_{0,ph}}{[M]_{ph}}\right) = k_p[R]_{ph}t \tag{3}$$

Figure 1 shows the conversion−time data for some of the photopolymerization experiments initiated by DMPA and MMMP at 25 °C. The resulting plots were adequately fitted by straight lines from the slopes of which $[R]_{ph}$ can be derived just by knowing the k_p value at this temperature (327 L mol^{-1} s^{-1}).[28] The obtained values are listed in Tables 1 and 2 for DMPA-initiated and MMMP-initiated polymerizations, respectively.

The stationary radical concentration was found to be higher in the DMPA-initiated photopolymerizations than in those initiated by MMMP at the same concentration. This obviously results in a higher polymerization rate when DMPA is using as photoinitiator. As one can expect, the $[R]_{ph}$ increases as the initiator concentration does so. This increase is, however, gentler at high initiator concentrations due probably to radical quenching. On the other hand, the $[R]_{ph}$ during the photopolymerization of MMA is 3-fold lower than the value obtained for butyl methacrylate (BMA) and 5-fold lower than in the case of dodecyl methacrylate (DMA); both monomers polymerizations under identical reaction conditions as those used in this work.[23] This fact gives an indication of the high $\langle k_t \rangle$ value associated with the bulk MMA polymerization in comparison to those observed for other alkyl methacrylates.

Postpolymerization in the Dark after UV Photoinitiation. After the disruption of the steady-state conditions by switching off the UV source, the monomer concentration in the dark was monitored by FT-IR during long periods of time. Some representative examples of the observed changes in monomer conversion as a function of time for experiments with DMPA and MMMP are plotted in Figures 2 and 3, respectively.

As can be observed in these figures, the polymerization reaction in the dark proceeded during long times rendering outstanding conversions, x_{dark}, regardless of the type of initiator (and the monomer conversion during the previous photopolymerization, x_{ph}). This result indicates that the radical concentration after stopping the production of primary radicals from the initiator is by no means negligible. A captious question can be posed as to whether the photoinitiators are able to decompose into primary radicals and initiate the polymerization in the dark. In general, the rates of initiation of the photoinitiators during dark period are genuinely considered as negligible or simply null. However, given the long-time experiments carried out in this work, an experimental check of this statement is mandatory. Several blank experiments were performed with both photoinitiators at different concentrations and skipping the initial photopolymerization. The monomer concentration was monitored by FTIR during long periods of time in a similar fashion as was done during regular experiments. Neither monomer conversion nor the presence of polymer after precipitation of the solution was observed in any of these blank experiments. Therefore, the MMA dark polymerization must be ascribed to the existence of long-lived radicals which persist after switching off the UV source, as was observed for other methacrylic monomers.[23]

Concerning the dark polymerization kinetics, the DMPA-initiated polymerizations (Figure 2) seem to be more dependent on the x_{ph} than those experiments in which the photoinitiator was MMMP (Figure 3). More information on kinetic parameters can be obtained from the analysis of the conversion−time curves according to the equations below.

The dark-time polymerization rate can also be described by the usual equation for steady-state conditions

$$-\frac{d[M]}{dt} = k_p[R][M] \tag{4}$$

where [M] and [R] account for the monomer and the radical concentrations, respectively, during the dark time. Since the rate of initiation during the postpolymerization is null, the time evolution of the radical concentration is on its turn given by eq 5

$$-\frac{d[R]}{dt} = \langle k_t \rangle [R]^2 \tag{5}$$

(Note the absence of factor 2 in the second term of eq 5 for better comparison with the results from previous work.[23]) The integrated equation that can be derived from eqs 4 and 5 reads

$$\frac{[M]_0}{[M]} = (1 + \langle k_t \rangle [R]_0 t)^{k_p/\langle k_t \rangle} \tag{6}$$

where $[M]_0$ and $[R]_0$ are the initial monomer and radical concentrations, respectively, after switching off the light. To obtain eq 6, the assumptions of time-invariant k_p and $\langle k_t \rangle$ are made. This is true for k_p since the existence of very small propagating radicals during the postpolymerization is not expectable. On the contrary, as k_t is essentially chain length dependent, the assumption of time-independent k_t involves that rendered $\langle k_t \rangle$ values will represent the average termination rate coefficient of the persistent radicals during the postpolymerization in the dark.

According to eq 6, the nonlinear curve fitting of the monomer conversion data shown in Figures 2 and 3 allowed to determine the coupled parameter values $\langle k_t \rangle [R]_0$ and $k_p/\langle k_t \rangle$ values for each postpolymerization experiment. As an example, the resulting fitting curves of the data plotted in Figures 2 and 3 are included in the graphs. By having k_p at hand,[28] the individual $\langle k_t \rangle$ and $[R]_0$ values were estimated from the afore described products. The as-obtained values of $[R]_0$ and $\langle k_t \rangle$ are gathered in Tables 1 and 2 for DMPA-initiated and MMMP-initiated experiments, respectively.

Table 1. Experimental Information and Results for the 2,2-Dimethoxy-2-phenylacetophenone (DMPA)-Initiated Polymerization Experiments of Methyl Methacrylate[a]

entry	[DMPA]/ (mol L^{-1})	x_{ph}	x_{dark}	$10^6[R]_{ph}$/ (mol L^{-1})	$\langle k_t \rangle$/ (L mol^{-1} s^{-1})	$10^8[R]_0$/ (mol L^{-1})	$DP_{n,ph}$	$DP_{n,dark}$	$DP_{n,initial}$	10^4C
1	0.008	0.05		0.53			190			
2	0.008	0.05	0.03	0.53	2346	0.98	181	4841	945	2.92
3	0.008	0.07	0.05	0.53	5804	1.27	163	4812	1032	3.19
4	0.008	0.08	0.21	0.53	419	0.52	162	8558	1305	1.68
5	0.03	0.05		1.06			161			
6	0.03	0.05	0.06	1.06	643	1.01	89	3581	561	3.44
7	0.03	0.05	0.11	1.06	4694	1.29	81	3804	543	3.10
8	0.03	0.05	0.12	1.06	3109	1.30	67	3682	514	3.23
9	0.03	0.05	0.25	1.06	4107	1.38	69	5550	598	2.29
10	0.03	0.09	0.07	1.06	7513	1.95	96	3335	573	3.91
11	0.03	0.18	0.09	1.06	2152	1.55	96	2800	711	5.49
12	0.03	0.27	0.13	1.06	2281	2.71	105	2649	819	6.93
13	0.10	0.03	0.11		1573	0.59	63	6433	704	2.07

[a] Photoinitiator concentration, [DMPA], monomer conversion and radical concentration during the photopolymerization, x_{ph} and $[R]_{ph}$, respectively, monomer conversion during the postpolymerization, x_{dark}, radical concentration at the beginning of the postpolymerization, $[R]_0$, average termination rate coefficient during postpolymerization, $\langle k_t \rangle$, number-average degrees of polymerization for the polymers obtained during the photopolymerization and the postpolymerization, $DP_{n,ph}$ and $DP_{n,dark}$, respectively, number-average degree of polymerization for the persistent radicals at the beginning of the postpolymerization, $DP_{n,initial}$, slope of the linear fit of the semilogarithmic plots of the chain length number fraction as a function of chain length in the high molecular weight region, *C*.

Table 2. Experimental Information and Results for the 2-Methyl-4′-(methylthio)-2-morpholinopropiophenone (MMMP)-Initiated Polymerization Experiments of Methyl Methacrylate[a]

entry	[MMMP]/ (mol L^{-1})	x_{ph}	x_{dark}	$10^6[R]_{ph}$/ (mol L^{-1})	$\langle k_t \rangle$/ (L mol^{-1} s^{-1})	$10^8[R]_0$/ (mol L^{-1})	$DP_{n,ph}$	$DP_{n,dark}$	$DP_{n,initial}$	10^4C
14	0.02	0.02	0.02	0.57	11632	1.40	179	6466	1193	2.59
15	0.02	0.03	0.07	laser	350	0.26		5960	1055	2.50
16	0.02	0.04	0.04	0.57	7042	0.77	234	6417	1220	2.48
17	0.02	0.04	0.09	0.57	2335	0.51	196	6956	1179	2.24
18	0.02	0.04	0.12	0.57	18782	1.62	114	9849	1055	1.30
19	0.02	0.04	0.52	0.57	3098	0.50	134	11197	1010	1.10
20	0.02	0.08		0.57			230			
21	0.02	0.08	0.02	0.57	14650	1.17	170	8161	1511	2.03
22	0.02	0.08	0.04	0.57	8706	0.87	216	9474	1600	1.65
23	0.02	0.08	0.05	0.57	32745	2.21	211	9939	1564	1.54
24	0.02	0.08	0.06	0.57	12068	0.95	174	8423	1380	1.81
25	0.02	0.08	0.17	0.57	1642	0.23	189	9845	1304	1.41
26	0.02	0.08	0.31	0.57	3450	0.43	300	11158	1166	1.17
27	0.02	0.12	0.05	0.57	10388	1.27	185	7193	1396	2.37
28	0.02	0.12	0.09	0.57	6340	0.99	175	6919	1334	2.36
29	0.02	0.15	0.03	0.57	5249	0.86	196	6947	1754	2.67
30	0.02	0.24		0.57			198			
31	0.02	0.24	0.06	0.57	<100	0.72	221	6719	1902	2.80
32	0.02	0.24	0.17	0.57	<100	0.56	221	6432	1618	2.73
33	0.02	0.24	0.24	0.57	<100	0.98	235	6502	1675	2.77
34	0.03	0.05	0.02	0.72	1200	0.57	138	6058	1444	2.80
35	0.03	0.18		0.72			167			
36	0.03	0.18	0.10	0.72	1022	1.36	141	3770	977	4.17
37	0.10	0.03	0.05	0.78	23430	0.58	144	11067	1247	1.15
38	0.10	0.08	0.07	0.78	5678	0.42	133	7941	1115	1.86

[a] Photoinitiator concentration, [MMMP], monomer conversion and radical concentration during the photopolymerization, x_{ph} and $[R]_{ph}$, respectively, monomer conversion during the postpolymerization, x_{dark}, radical concentration at the beginning of the postpolymerization, $[R]_0$, average termination rate coefficient during postpolymerization, $\langle k_t \rangle$, number-average degrees of polymerization for the polymers obtained during the photopolymerization and the postpolymerization, $DP_{n,ph}$ and $DP_{n,dark}$, respectively, number-average degree of polymerization for the persistent radicals at the beginning of the postpolymerization, $DP_{n,initial}$, slope of the linear fit of the semilogarithmic plots of the chain length number fraction as a function of chain length in the high molecular weight region, *C*.

The $[R]_0$ values scarcely exceed 2×10^{-8} mol L^{-1}, and they are generally higher for DMPA-initiated polymerizations than for those initiated by MMMP. However, there is no influence of the initiator concentration on the $[R]_0$ values. In addition, these values in the DMPA-initiated experiments show the trend to increase as x_{ph} does so, whereas the same trend in MMMP-initiated experiments is not straightforward. These results are consistent with the higher radical concentration detected during the photopolymerization for the DMPA-initiated reactions and also explain why DMPA-initiated experiments in the dark are more dependent on x_{ph}. In comparison with the results obtained for other alkyl methacrylates,[23] the estimated $[R]_0$ values in the postpolymerization of MMA are more than 7-fold lower than in the postpolymerization of BMA and even 1 order of magnitude lower than in the case of the postpolymerization of DMA under identical conditions. This also agrees with the results obtained during the photopolymerization time.

However, the $\langle k_t \rangle$ values obtained from the fitting procedure with the conversion data during the postpolymerization of MMA are very similar to those previously reported for BMA and DMA. Therefore, the well-known dependency of the alkyl chain length on the $\langle k_t \rangle$ values is not detected in these postpolymerization reactions. This fact is explained by the nature of the propagating radicals in the postpolymerization period: no primary radicals are produced, and only long-chain radicals persist. Under such conditions the alkyl chain of the monomer

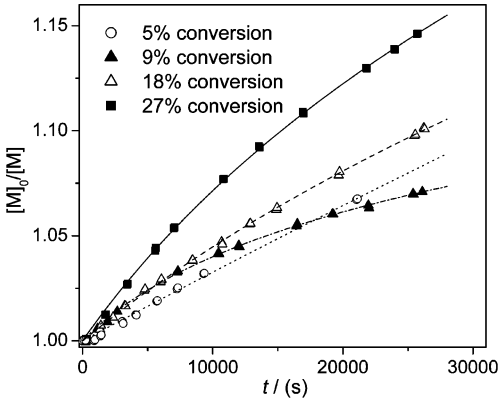

Figure 2. Changes in monomer concentration with time for methyl methacrylate bulk polymerization in the dark after 2,2-dimethoxy-2-phenylacetophenone (DMPA)-initiated photopolymerization in which the monomer conversions were 5, 9, 18, and 27% (entries 6, 10, 11, and 12 in Table 1). The initial DMPA concentration was 3×10^{-2} mol L^{-1}. The lines represent the best fits for the experimental data according to eq 6.

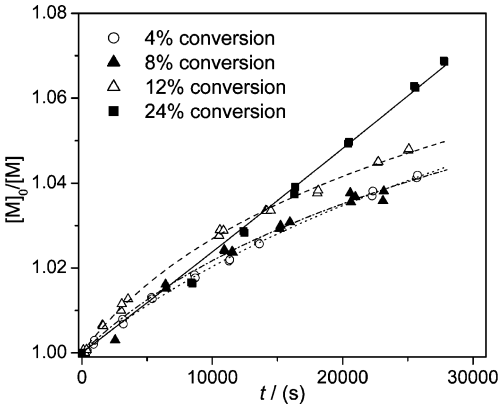

Figure 3. Changes in monomer concentration with time for methyl methacrylate bulk polymerization in the dark after 2-methyl-4′-(methylthio)-2-morpholinopropiophenone (MMMP)-initiated photopolymerization in which the monomer conversions were 4, 8, 12, and 24% (entries 16, 22, 27, and 31 in Table 2). The initial MMMP concentration was 2×10^{-2} mol L^{-1}. The lines represent the best fits for the experimental data according to eq 6.

entity cannot play an important role on the radical diffusion rate and, hence, on the termination rate coefficient.

In addition, the $\langle k_t \rangle$ values listed in Tables 1 and 2 are rarely larger than 10^4 L mol^{-1} s^{-1}. Given the relative low x_{ph} values, a relationship between this parameter and the $\langle k_t \rangle$ values obtained cannot be directly assigned but can be suspected. However, the experiments in which large x_{dark} were achieved clearly show a distinct behavior associated with the variation of $\langle k_t \rangle$ with monomer conversion. In this connection, Figure 4 shows some experiments where the reactions in the dark were let to proceed up to conversions higher than 20%.

Up to roughly 10% conversion, the reactions in the dark time shown in Figure 4 proceeded in a similar fashion as those shown in Figures 2 and 3. For approximately the same x_{ph}, DMPA-initiated experiment (entry 9 in Table 1, Figure 4) exhibited a higher polymerization rate than the experiment initiated by MMMP (entry 26 in Table 2, Figure 4) due to the lower $[R]_0$ value of the latter. The same happens when comparing both MMMP-initiated experiments (entries 26 and 33 in Table 2, Figure 4) at different x_{ph}: the higher the x_{ph}, the larger the $[R]_0$ and, hence, the higher the polymerization rate. However, a sharp increase in the polymerization rate over 10% conversion in the dark time, i.e., an autoaccelaration phenomenon, is a common

Table 3. Experimental Information and Results for the Azobis(isobutyronitrile) (AIBN)-Initiated Polymerization Experiments of Methyl Methacrylate[a]

entry	[AIBN]/(mol L^{-1})	x_{ph}	x_{th}	$10^8[R]_{th}$/(mol L^{-1})	$DP_{n,ph}$	$DP_{n,th}$	10^4C
39	0.01	0.03	0.03	0.18	425	24244	0.40
40	0.01	0.03	0.05	0.23	419	25766	0.37
41	0.03	0.04	0.04	0.42	242	15182	0.87
42	0.03	0.04	0.06	0.38	258	14886	0.74
43	0.05	0.04	0.02	0.61	260	11053	1.37
44	0.10	0.04	0.04	0.84	216	8843	1.78
45	0.10	0.04	0.31	0.93	167	10843	0.99
46	0.25	0.03	0.04	1.20	170	7192	2.12
47	0.25	0.03	0.18	1.27	105	8342	1.49
48	0.32	0.02	0.03	1.59	187	6616	2.39
49	0.32	0.02	0.23	1.52		12297	
50	0.45	0.02	0.06	1.67	172	6000	2.55

[a] Initiator concentration, [AIBN], monomer conversion during the photopolymerization, x_{ph}, monomer conversion during the thermal polymerization, x_{th}, radical concentration during the thermal polymerization, $[R]_{th}$, number-average degrees of polymerization for the polymers obtained during the photopolymerization and the thermal polymerization, $DP_{n,ph}$ and $DP_{n,th}$, respectively, slope of the linear fit of the semilogarithmic plot of the chain length number fraction as a function of chain length in the high molecular weight region, C.

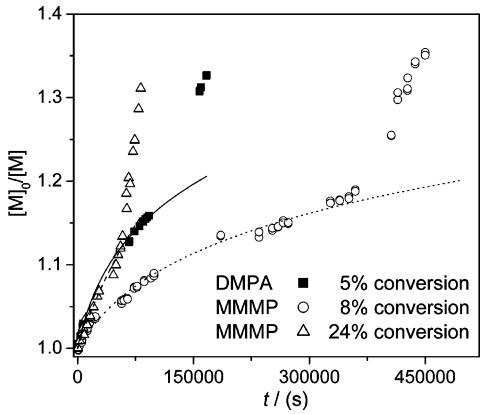

Figure 4. Changes in monomer concentration with time for methyl methacrylate bulk polymerization in the dark up to high conversions (entry 9 in Table 1 and entries 26 and 33 in Table 2). The initiator type and the conversion during the photopolymerization time are given within the figure. The lines represent the best fits for the experimental data (only considered up to 10% conversion) according to eq 6.

feature for the three experiments depicted in Figure 4. This increase must be ascribed to a lowering in $\langle k_t \rangle$ as the reaction proceeds, mainly caused by a progressive rise in the viscosity of the medium. Actually, evaluations of eq 6 for assumed $\langle k_t \rangle$ values lower than k_p would render such a continuous increase in the polymerization rate, which is an additional indication of the genuineness of the behavior during the dark period.

At this point, it must be noticed that the laser-initiated reaction (entry 15 in Table 2) could be said to exhibit a lower $[R]_0$ value than an analogous experiment initiated by the UV lamp (see as example entry 17 in Table 2). This could be due to the narrower radical size distribution produced by the laser initiation, but in essence, both initiation sources led to similar results during the postpolymerization.

On the other hand, the radical average half-lifetimes, τ, derived from the inverse of the product $\langle k_t \rangle [R]_0$ are extremely long, which will obviously result in very high molecular weight materials produced during the dark period. Before discussing this point, it is worth analyzing the kinetics of the MMA polymerization with a continuous primary radical generation (i.e., thermally initiated) at the same temperature at which the postpolymerization reactions were carried out.

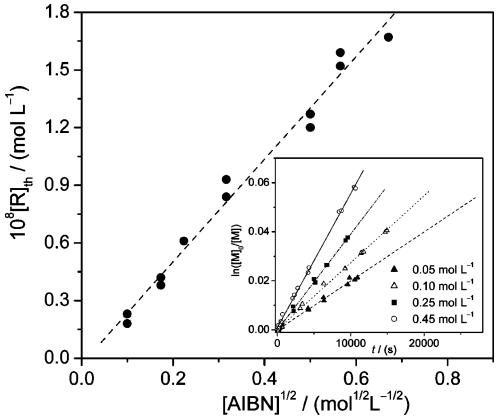

Figure 5. Square root dependence of the radical concentration under steady-state conditions, $[R]_{th}$, on the azobis(isobutyronitrile) (AIBN) concentration. Plotted in the inset are some examples of conversion−time data from which the $[R]_{th}$ were derived (entries 43, 44, 46, and 50 in Table 3).

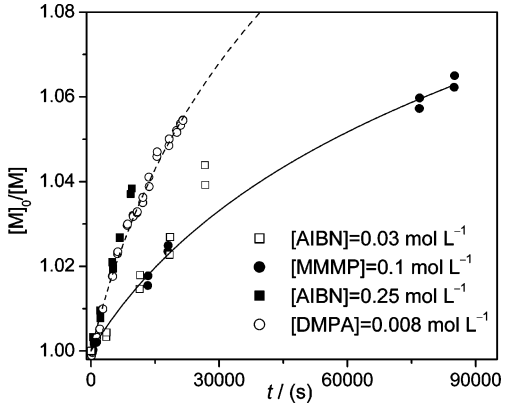

Figure 6. Changes in monomer concentration with time for methyl methacrylate postpolymerization and thermally initiated polymerization (entry 3 in Table 1, entry 38 in Table 2, and entries 41 and 46 in Table 3). The initiator type and initial concentration are given within the figure. The lines represent the best fits for the experimental data according to eq 6.

Thermal Polymerization. The low $[R]_0$ values rendered by the fitting procedure preclude a radical detection by conventional methods such as EPR.[23] Nevertheless, to check the reliability of the fitting, similar radical concentrations as those found during postpolymerization can be achieved under steady-state conditions using a thermal initiator. Then, to study the differences, if any, between steady-state and postpolymerization conditions, some experiments with AIBN concentrations ranging from 1×10^{-2} to 0.45 mol L^{-1} were carried out. For a better comparison, the AIBN-initiated reactions were also subjected to a previous photoinitiated period, but only up to very low conversions (no more than 4%). Experimental conditions and results from the thermal polymerizations are listed in Table 3. The thermal polymerization experiments were designed to provide steady-state radical concentrations, $[R]_{th}$, within the range found for the $[R]_0$ in the postpolymerization reactions.

The steady-state assumption leads to the following equation

$$[R]_{th} = \left(\frac{2fk_d[I]}{\langle k_t\rangle_{th}}\right)^{1/2} \quad (7)$$

were f, k_d, and [I] are the efficiency, the decomposition rate constant, and the concentration of the initiator, respectively. $\langle k_t\rangle_{th}$ in eq 7 refers to the average termination rate coefficient under steady-state conditions. Therefore, the radical concentration under steady-state conditions is linearly dependent on the square root of the initiator concentration. This dependence is confirmed for the thermal polymerizations performed in this work and shown in Figure 5. According to eq 3, the $[R]_{th}$ values were obtained from the slopes of the lines resulting of fitting conversion−time plots (some examples are shown in the inset of Figure 5). The so-obtained radical concentrations are listed in the fifth column of Table 3. As intended, these values are of the same order as the $[R]_0$ obtained in the postpolymerization experiments (lower than 2×10^{-8} mol L^{-1}), but in the AIBN-initiated experiments, they have been achieved by a continuous generation of primary radicals from the initiator.

In addition, from the slope obtained by the linear fit of the data plotted in Figure 5, a $\langle k_t\rangle_{th}$ value for the thermal polymerizations can be estimated. Assuming $f = 0.5$ and $k_d = 5.58 \times 10^{-8}$ s^{-1} at 25 °C (both values extracted from the literature[29]), $\langle k_t\rangle_{th} = 7.84 \times 10^7$ L mol^{-1} s^{-1} is obtained, a value which is in agreement with others found in the literature[30] (note again the absence of factor 2 for describing the termination rate).

On the other hand, the comparison between thermally initiated and the postpolymerization reactions is shown in Figure 6. To build this figure, two pairs of experiments in which both $[R]_{th}$ and $[R]_0$ were practically identical were chosen. As before stated, the $[R]_0$ values for the postpolymerization reactions are independent of the initiator concentration; the opposite occurs in the thermally initiated polymerization. The changes in monomer concentration during postpolymerization are adequately fitted by eq 6, whereas straight lines (obviously only up to such low conversions as shown in Figure 5) described the changes in monomer concentration during thermally initiated polymerizations. This is so because there is a progressive diminishing in the radical concentration during postpolymerization, whereas thermally initiated reactions proceed under steady-state conditions.

However, what is really remarkable from the observation of Figure 6 is that the polymerization rates at low conversions for thermally initiated and postpolymerization reactions are very similar when comparing experiments in which $[R]_{th}$ and $[R]_0$ are identical, regardless of their actual values. This fact strongly suggest that the fitting procedure used in the postpolymerizations provides reliable $[R]_0$ values, and therefore, the $\langle k_t\rangle$ values listed in Tables 1 and 2 are not far for reality. The implications which these extremely low values for $\langle k_t\rangle$ have in conventional free radical kinetics will be discussed in a forthcoming section.

Molecular Weight Distributions. The peculiar reaction conditions during the postpolymerization experiments will presumably produce high molecular weight pMMA. The number-average degree of polymerization for the fraction of polymer yielded during the initial photoinitiated reaction, $DP_{n,ph}$, and during the dark period, $DP_{n,dark}$, are both gathered in Tables 1 and 2. All the samples exhibited bimodal MWD pattern induced by these two polymerization regimes. The polymers synthesized during the first stage exhibit number-average molecular weights which are controlled by the initiator concentration, whereas the polymers obtained during the second stage (postpolymerization time) show no trend with initial initiator concentration and are outstandingly high as a rule. Some MWD corresponding to different experiments are depicted in Figures 7 and 8. Shared features of the resulting materials obtained during the postpolymerization reactions can be deduced from these figures: (i) MMMP-initiated experiments generally rendered higher molecular weight materials than those initiated by DMPA, (ii) the higher the conversion during postpolymerization, the higher the molecular weight of the resulting polymer,

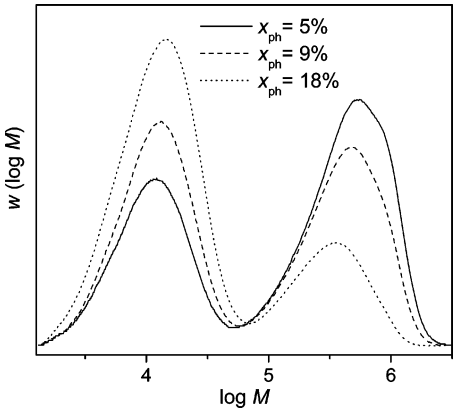

Figure 7. Molecular weight distributions of the polymers obtained after 2,2-dimethoxy-2-phenylacetophenone (DMPA)-initiated experiments in which the initial monomer conversions during the photopolymerization time, x_{ph}, were 5, 9, and 18% (entries 6, 10, and 11 in Table 1). The conversions during the postpolymerizations vary for each experiment.

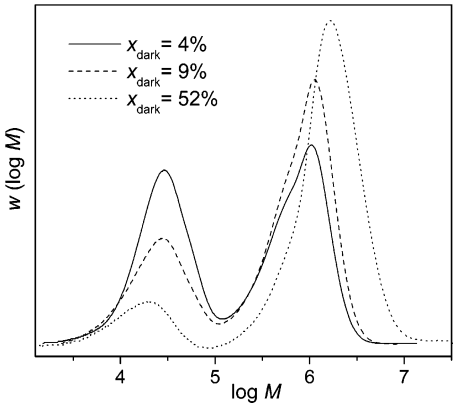

Figure 8. Molecular weight distributions of the polymers obtained after 2-methyl-4′-(methylthio)-2-morpholinopropiophenone (MMMP)-initiated experiments in which the monomer conversions during the postpolymerization, x_{dark}, were 4, 9, and 52% (entries 16, 17, and 19 in Table 2). The conversion during the initial photopolymerization was 4% for the three samples.

and (iii) the higher the conversion during the initial photopolymerization period, the lower the molecular weight of the polymer obtained during the dark period. These observations can adequately explain in terms of the differences found in the $[R]_0$ values. However, a comparison between experiments with similar $[R]_0$ values but different initiators provides further information.

The number-average degrees of polymerization for the polymers obtained from AIBN-initiated experiments, $DP_{n,th}$, are also listed in Table 3. The sixth column of this table shows also the number-average degrees of polymerization corresponding to the fraction of polymer obtained during the first photoinitiated period, $DP_{n,ph}$. The molecular weights of the polymers obtained by thermal polymerizations are dependent on the initiator concentration as usually occurs: the highest molecular weight materials (DP_n higher than 24 000) are obtained at low AIBN concentrations. Then, a comparison of the three initiators must be done on the basis of similar radical concentrations for all the experiments (initial radical concentration, $[R]_0$, in the postpolymerization reactions).

Figure 9 shows three MWD of samples obtained after postpolymerizations initiated by both DMPA and MMMP with similar $[R]_0$ values and a thermal polymerization which exhibited a comparable $[R]_{th}$. Under these conditions, the molecular weight

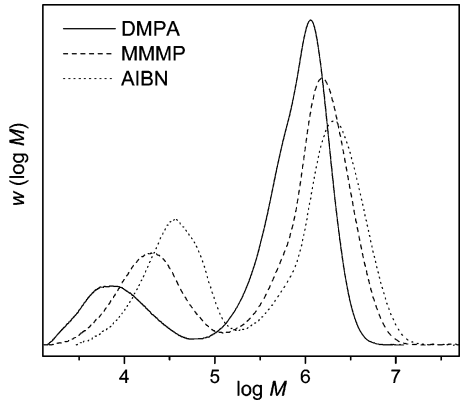

Figure 9. Molecular weight distributions of the polymers obtained after a 2,2-dimethoxy-2-phenylacetophenone (DMPA)-initiated postpolymerization experiment (entry 13 in Table 1), a 2-methyl-4′-(methylthio)-2-morpholinopropiophenone (MMMP)-initiated postpolymerization experiment (entry 37 in Table 2), and an azobis(isobutyronitrile) (AIBN)-initiated thermal polymerization (entry 42 in Table 3).

of the polymer obtained by thermal polymerization is clearly higher than those yielded by the postpolymerization experiments. This assessment can be extended to the rest of the experiments. Given that the reaction conditions are identical, the differences found in the molecular weights of the yielded polymers must mainly be ascribed to the occurrence of transfer reactions to the initiator. The transfer reactions to the monomer are supposed to be of the same extent for all the experiments independently on the initiator type. The same occurs with transfer reaction to the polymer, although this will not be considered in the rest. This assumption is based on the fact that transfer reactions to the polymer are not expected at such low monomer conversions. Besides, the good agreement found between the fraction of polymer synthesized during the postpolymerization obtained by the SEC analysis and the experimental conversion measured by FTIR suggests that only high molecular weight chains are generated during the dark time. Therefore, although the transfer reactions to the polymer cannot be strictly ruled out, they can be considered as negligible for the analysis.

On the other hand, to carry out the analysis of the transfer reactions, the term $DP_{n,initial}$ has been defined. As discussed in our previous work,[23] this term refers to the number-average degree of polymerization for the radicals which survive after stopping the continuous generation of primary radicals from the initiator. Although shortcomings are involved to the assignation of $DP_{n,initial}$, it can be assumed that this value is close to the intersection point between the two MWD which give rise to the bimodal patterns. The corresponding values extracted from the SEC traces are included in Tables 1 and 2.

Transfer Reactions. The kinetic analysis of the reaction and the quantitative values of the polymer molecular weights can provide valuable information on the initial and instantaneous radical concentration during the postpolymerization. In our previous paper,[23] a kinetic analysis of the postpolymerization reactions and the influence of living and dead chains (generated by transfer or bimolecular termination reactions) on the $DP_{n,dark}$ were profusely described.

In bulk polymerization at low conversions, the transfer reactions to the monomer are supposed to have more contribution than the transfer reactions to the polymer or the initiator. However, as stated above, the experimental evidence found for the bulk polymerization of MMA initiated by either DMPA or MMMP seems to indicate that the transfer reactions to the initiator play also a decisive role.

Assuming the contribution of transfer reactions to the polymer as negligible, the rate of formation of dead polymer chains generated by transfer reactions, $[R]_{dead}$, is given by

$$\frac{d[R]_{dead}}{dt} = k_{tr_M}[R][M] + k_{tr_I}[R][I] \quad (8)$$

where k_{tr_M} and k_{tr_I} are the transfer rate constants to the monomer and the initiator, respectively. The integration of eq 8 renders the $[R]_{dead}$ value

$$[R]_{dead} = C_M([M]_0 - [M]) + [I]_0\left(1 - \left(\frac{[M]_0}{[M]}\right)^{-C_I}\right) \quad (9)$$

defining the transfer constants to the monomer and to the initiator, C_M and C_I, respectively, as the ratio of the transfer rate constants, k_{tr_M} and k_{tr_I}, to the propagation rate, k_p.

The number-average molecular weight is then given by eq 10

$$DP_{n,dark} = \frac{[M]_0 - [M]}{\left(\frac{2-\alpha}{2}\right)[R]_0 + \frac{\alpha}{2}[R] + [R]_{dead}} + DP_{n,initial} \quad (10)$$

where α is the fraction of termination by coupling reactions. Knowing that $[R]_0$ and, thus, [R] are both extremely low, the $DP_{n,dark}$ is almost exclusively controlled by $[R]_{dead}$:

$$DP_{n,dark} \approx \frac{[M]_0 - [M]}{[R]_{dead}} + DP_{n,initial} \quad (11)$$

The combination of eqs 9 and 11 reads

$$\frac{[M]_0 - [M]}{DP_{n,dark} - DP_{n,initial}} = C_M([M]_0 - [M]) + [I]_0\left(1 - \left(\frac{[M]_0}{[M]}\right)^{-C_I}\right) \quad (12)$$

The method outlined by Clay et al.[31] to determine the transfer constant to the monomer based on the instantaneous chain length distribution (CLD) analysis can be applied if (i) the transfer to the monomer is favored over other termination mechanisms and (ii) high molecular weights are obtained. In the case of the postpolymerization experiments, both criteria are fulfilled, but a nonnegligible transfer to the initiator has been detected. Under these circumstances, the instantaneous number fraction distribution of the polymer chains, $N_i = w(\log i)/i^2$, must be defined as[32]

$$N_i = \exp(-iC) \quad (13)$$

where C will be given by

$$C = C_M + \frac{[I]_0\left(1 - \left(\frac{[M]_0}{[M]}\right)^{-C_I}\right)}{[M]_0 - [M]} \quad (14)$$

Therefore, the C values for every postpolymerization experiment can be directly extracted from the slopes of the straight lines obtained by the semilogarithmic plots of the chain length number fraction as a function of chain length. As an example, Figure 10 shows such a semilogarithmic plot for the SEC traces depicted in Figure 9. The C values are determined from the slopes of the straight lines within the high molecular weight range, as marked in the inset of Figure 10 for the SEC trace

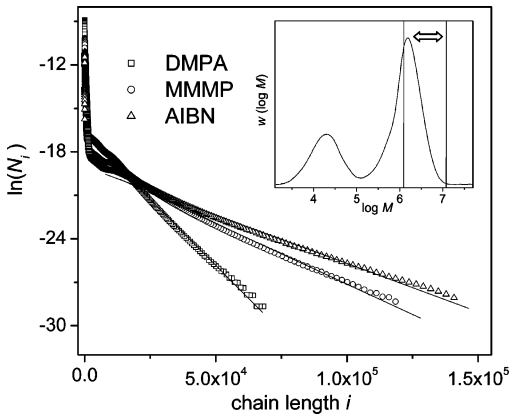

Figure 10. Semilogarithmic plot of the chain length number fraction as a function of chain length for the polymers obtained after a 2,2-dimethoxy-2-phenyl-acetophenone (DMPA)-initiated postpolymerization experiment, a 2-methyl-4′-(methylthio)-2-morpholinopropiophenone (MMMP)-initiated postpolymerization experiment, and an azobis(isobutyronitrile) (AIBN)-initiated thermal polymerization (entry 13 in Table 1, entry 37 in Table 2, and entry 42 in Table 3). Plotted in the inset is the SEC trace corresponding to the polymer yielded during the MMMP-initiated experiment showing the range of molecular weight for which C (slopes of the linear fits included in the figure) is determined.

corresponding to the MMMP-initiated experiment. The C values obtained so are listed in the last columns of Tables 1 and 2.

An identical procedure can be applied for the polymers synthesized by thermal polymerizations. In the case of the AIBN-initiated reactions, the number-average molecular weight under steady-state conditions, $DP_{n,th}$, is defined by eq 15, which takes into account the bimolecular termination reactions and the transfer reactions to the monomer and to the initiator:

$$DP_{n,th} = \{[M]_0 - [M]\}/\left\{C_M([M]_0 - [M]) + f(2-\alpha)([I]_0 - [I]) + \frac{2}{3}C_I k_p\left(\frac{2f}{k_t k_d}\right)^{1/2}([I]_0^{3/2} - [I]^{3/2})\right\} \quad (15)$$

Then, the above-described term C will be now given by eq 16.

$$C = C_M + f(2-\alpha)\frac{[I]_0 - [I]}{[M]_0 - [M]} + \frac{2}{3}C_I k_p\left(\frac{2f}{k_t k_d}\right)^{1/2}\frac{[I]_0^{3/2} - [I]^{3/2}}{[M]_0 - [M]} \quad (16)$$

The semilogarithmic plots can also be drawn with the SEC traces of the polymers obtained by the thermal polymerizations, and the C values can be estimated from the slopes of the straight lines within the high molecular weight range. An example of this (corresponding to the SEC trace depicted in Figure 9) is included in Figure 10. The so-obtained C values are collected in the last column of Table 3.

The C values for the postpolymerization experiments (Tables 1 and 2) as well as those for the thermal polymerizations (Table 3) are dependent on the molecular weight of the polymer. Actually, as can be deduced from eqs 11–16, the transfer constant to the monomer can be determined by plotting the C values as a function of the inverse of either $(DP_{n,dark} - DP_{n,initial})$ for the postpolymerizations or $DP_{n,th}$ for the thermal polymerizations. Figure 11 shows such plots for the C values obtained from the MMMP-initiated postpolymerization experiments and from the thermal polymerizations. As can be seen in this figure,

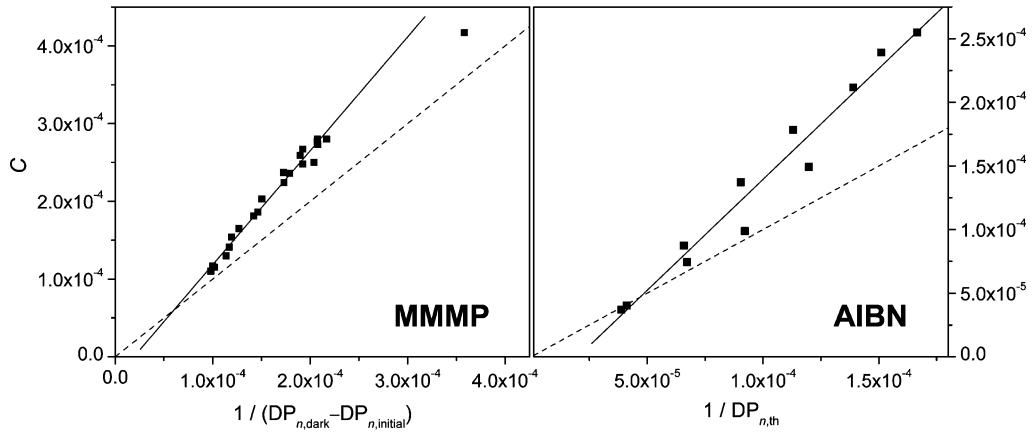

Figure 11. Plots of the *C* values as a function of the inverse of either the difference between the number-average degree of polymerization for the polymers obtained during the 2-methyl-4′-(methylthio)-2-morpholinopropiophenone (MMMP)-initiated postpolymerization experiments, $DP_{n,dark}$, and the number-average degree of polymerization for the persistent radicals at the beginning of these postpolymerization reactions, $DP_{n,initial}$ (left), or the number-average degree of polymerization for the polymers obtained during the azobis(isobutyronitrile) (AIBN)-initiated thermal polymerizations, $DP_{n,th}$ (right). Solid lines are the linear fits of the data. Dashed lines represent the lines of slope unity.

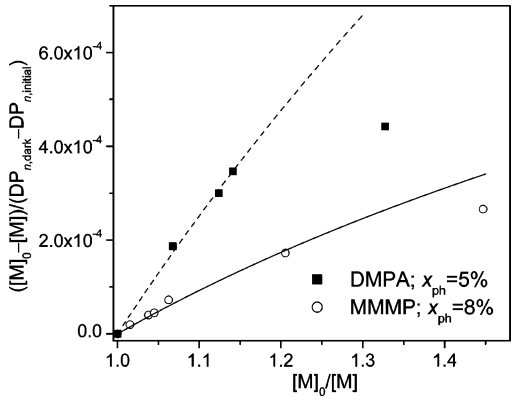

Figure 12. Plots of the conversion dependent differences in monomer concentration divided by the differences between the number-average degree of polymerization for the polymers obtained during the postpolymerizations, $DP_{n,dark}$, and the number-average degree of polymerization for the persistent radicals at the beginning of these postpolymerization reactions, $DP_{n,initial}$. The initial conversion during the photopolymerization time, x_{ph}, for the 2,2-dimethoxy-2-phenylacetophenone (DMPA)-initiated polymerizations (entries 6−9 in Table 1) is 5% and for the 2-methyl-4′-(methylthio)-2-morpholinopropiophenone (MMMP)-initiated polymerization experiments $x_{ph} = 8\%$ (entries 21−26 in Table 2). The lines are the best fits of the data according to eq 12.

the *C* values are fairly well fitted as straight lines (solid lines in the figure), the intersections of which with the lines of slope unity (dashed lines in the figure) will render the C_M values. Thus, the C_M values deduced from Figure 11 are 6.0×10^{-5} for the MMMP-initiated postpolymerizations and 4.7×10^{-5} for the thermal polymerizations. These values for C_M at 25 °C are within the range of others found in the literature at different temperatures.[30,33,34] It must be noticed that the *C* values obtained at low $DP_{n,dark}$ are not laying on the same straight line as the rest (see MMMP-initiated experiments in Figure 11). This could be due to the errors made on assigning the $DP_{n,initial}$. This effect is also detected in the homologous plot with the *C* values determined from the DMPA-initiated experiments. Nevertheless, a lack of the linear dependence of the *C* values on $1/(DP_{n,dark} - DP_{n,initial})$ at wide $DP_{n,dark}$ range cannot be ruled out.

On the other hand, knowing the C_M value, the transfer constant to the initiator can be estimated by using eq 12 for the calculus. Figure 12 shows the plots of the first term of eq 12 as a function of $[M]_0/[M]$ for DMPA-initiated and MMMP-initiated postpolymerizations in which x_{ph} were identical for each data set (entries 6−9 in Table 1 and entries 21−26 in Table 2). The C_I values for the photoinitiators can be determined by fitting the data points according to eq 12. The fitting results are shown as lines in Figure 12, indicating that the data points are adequately simulated by means of this equation. The data which correspond to the experiments at large conversions during the dark time are out of the fitting. This effect can be attributed to the likely existence of transfer reactions to the polymer (at such high polymer concentrations in the medium) which have not been considered for the analysis.

The fitting procedure renders C_I values of 0.074 and 0.037 for DMPA and MMMP, respectively. As expected, DMPA shows a higher transfer rate compared to MMMP. Both photoinitiators are, in any case, far from being ideal if they are compared to AIBN in which null contribution of transfer reactions to primary radicals is reported ($C_I = 0$).[30] Knowing the C_I values for the three initiators used in this work, it is easy to understand why, under similar reaction conditions, the molecular weight of the resulting polymers follows the trend shown in Figure 9.

Termination Rate Coefficients. Once the transfer events have been assessed and studied, discussion of the $\langle k_t \rangle$ obtained values must be done. As shown in Tables 1 and 2 and stated above, the $\langle k_t \rangle$ values determined in this work are extremely low but in agreement with those found in our previous work for the postpolymerization reactions of BMA, DMA, and 3-[tris(trimethylsilyloxy)silyl]propyl methacrylate (TRIS).[23]

The "composite model" which describes the chain-length dependence of k_t in dilute solutions proposes $\beta \approx 0.16$ as the power-law exponent holding for long chains.[17] According to this model, the predicted k_t^{ii} value for two radicals of $DP_n = 1000$ will be roughly 7×10^7 L mol^{-1} s^{-1} (this value is obtained assuming $k_t^{1,1} = 10^9$ L mol^{-1} s^{-1}). In a polymerization system under non-steady-state conditions in which radicals of $1 \leq i \leq 1000$ are coexisting, the possible k_t^{ij} values will always be higher than this k_t^{ii}. This situation would ideally describe the initial conditions of our postpolymerization experiments (i.e., the conditions the moment the light is switched off). Thus, assuming the most unfavorable case, a radical concentration $[R]_{ph} = 10^{-6}$ mol L^{-1} would be reduced by 2 orders of magnitude after under 2 s, and after 60 s the radical concentration would be roughly 10^{-10} mol L^{-1}. These values would preclude the experimental detection of posteffects as those described for MMA, BMA, DMA, and TRIS. Then, power-law exponents within the range

of those proposed by the "composite model" cannot explain radical concentrations of 10^{-8} mol L^{-1} which persist 60 s after stopping the primary radical production.

We can make a very rough approximation and consider that the obtained $\langle k_t \rangle$ values could be assigned to k_t^{ii} for radicals of chain length ranging between $DP_{n,initial}$ and $DP_{n,dark}$. Even knowing that this situation is highly hypothetical, the power-law exponent to describe the chain-length dependency of k_t would range between 1.70 and 1.20. It is remarkable that for dense polymer media of high viscosity some theories predicted power-law exponent values ranging from 1 to 2.[5−7] Our results on the postpolymerization experiments suggest that, even at low conversions where no viscosity effects are expected, the persistent radicals are long enough to become entangled and show a very restricted mobility, which clearly precludes the bimolecular termination events. Therefore, the molecular weight of the resulting polymers is almost exclusively controlled by the transfer reactions.

Conclusions

The postpolymerization reaction of methyl methacrylate at 25 °C has proved to be a valuable experimental approach to obtain a deeper insight into the kinetics of free-radical polymerization systems. After a photoinitiated period which yields low monomer conversions, the primary radical production was cut off and the existence of persistent radicals propagating in the dark during long periods of time was checked. A quantitative analysis of the postpolymerization kinetics by a fitting procedure provided the average value of the termination rate coefficients, $\langle k_t \rangle$, and the radical concentrations during the posteffect. The reliability of these quantities was tested by carrying out thermal polymerizations under steady-state conditions but reproducing the polymerization rate of the experiments in the dark. The determined $\langle k_t \rangle$ values (usually lower than 10^4 L mol^{-1} s^{-1}) suggest that the power-law exponents that assess the chain-length dependency of k_t should be higher than the unity for long radicals even in dilute solution (i.e., at low monomer conversions). The molecular weights of the polymers obtained during the postpolymerization are essentially controlled by transfer reactions. A method, based on the analysis of the instantaneous chain length distribution,[31] to determine the transfer constants to the monomer and to the initiator is proposed. The value obtained for the transfer constant to the monomer is on average 5.5×10^{-5}, in good agreement with data from the literature. Regarding the transfer constant to the initiator, the C_I values for 2-phenylacetophenone (DMPA) and the 2-methyl-4′-(methylthio)-2-morpholinopropiophenone (MMMP) were determined. DMPA was found to act as a more efficient transfer agent in comparison to MMMP. In spite of the transfer events, the polymers obtained during these polymerization experiments are of extremely high molecular weight (DP_n even higher than 11 000 for MMMP-initiated experiments), which makes this method suitable to synthesize high molecular weight materials by conventional free-radical polymerization.

Acknowledgment. We acknowledge financial support from the Ministerio de Educación y Ciencia (Programa "Ramón y Cajal", CICYT-MAT2005-05648-C02-01 and CTQ2005-07860/BQU).

References and Notes

(1) Asua, J. M.; Beuermann, S.; Buback, M.; Castignolles, P.; Charleux, B.; Gilbert, R. G.; Hutchinson, R. A.; Leiza, J. R.; Nikitin, A. N.; Vairon, J.-P.; van Herk, A. M. *Macromol. Chem. Phys.* **2004**, *205*, 2151−2160 and the rest of the series cited therein.
(2) Buback, M.; Egorov, M.; Gilbert, R. G.; Kaminsky, V.; Olaj, O. F.; Russell, G. T.; Vana, P.; Zifferer, G. *Macromol. Chem. Phys.* **2002**, *203*, 2570−2582.
(3) Barner-Kowollik, C.; Buback, M.; Egorov, M.; Fukuda, T.; Goto, A.; Olaj, O. F.; Russell, G. T.; Vana, P.; Yamada, B.; Zetterlund, P. B. *Prog. Polym. Sci.* **2005**, *30*, 605−643.
(4) Benson, S. W.; North, A. M. *J. Am. Chem. Soc.* **1962**, *84*, 935−940.
(5) Cardenas, J.; O'Driscoll, K. F. *J. Polym. Sci., Polym. Chem. Ed.* **1976**, *14*, 883−897.
(6) Tulig, T. J; Tirrell, M. *Macromolecules* **1981**, *14*, 1501−1511.
(7) de Gennes, P. G. *J. Chem. Phys.* **1982**, *76*, 3322−3326.
(8) Soh, S. K.; Sundberg, D. C. *J. Polym. Sci., Polym. Chem. Ed.* **1982**, *20*, 1299−1313.
(9) Olaj, O. F.; Zifferer, G.; Gleixner, G. *Macromolecules* **1987**, *20*, 839−850.
(10) Mahabadi, H. K. *Macromolecules* **1985**, *18*, 1319−1324.
(11) Bamford, C. H. *Eur. Polym. J.* **1989**, *25*, 683−689.
(12) Zhu, S.; Tian, Y.; Hamielec, A. E.; Eaton, D. R. *Macromolecules* **1990**, *23*, 1144−1150.
(13) Russell, G. T.; Gilbert, R. G.; Napper, D. H. *Macromolecules* **1992**, *25*, 2459−2469.
(14) O'Shaughnessy, B.; Yu, J. *Macromolecules* **1994**, *27*, 5067−5078.
(15) Buback, M.; Kowollik, C. *Macromolecules* **1998**, *31*, 3211−3215.
(16) Vana, P.; Davis, T. P.; Barner-Kowollik, C. *Macromol. Rapid Commun.* **2002**, *23*, 952−956.
(17) Smith, G. B.; Russell, G. T.; Heuts, J. P. A. *Macromol. Theory Simul.* **2003**, *12*, 299−314.
(18) Buback, M.; Hippler, H.; Schweer, J.; Vögele, H. -P. *Makromol. Chem., Rapid Commun.* **1986**, *7*, 261−265.
(19) Buback, M.; Egorov, M.; Junkers, T.; Panchenko, E. *Macromol. Rapid Commun.* **2004**, *25*, 1004−1009.
(20) de Kock, J. B. L.; Klumpermann, B.; van Herk, A. M.; German, A. L. *Macromolecules* **1997**, *30*, 6743−6753.
(21) Johnston-Hall, G.; Stenzel, M. H.; Davis, T. P.; Barner-Kowollik, C.; Monteiro, M. J. *Macromolecules* **2007**, *40*, 2730−2736.
(22) Lovestead, T. M.; Theis, A.; Davis, T. P.; Stenzel, M. H.; Barner-Kowollik, C. *Macromolecules* **2006**, *39*, 4975−4982.
(23) García N.; Tiemblo, P.; Hermosilla, L.; Sieiro, C.; Guzmán, J. *Macromolecules* **2005**, *38*, 7601−7609.
(24) Beuermann, S.; Buback, M. *Prog. Polym. Sci.* **2002**, *27*, 191−254.
(25) Benoit, H.; Grubisic, Z.; Rempp, P.; Decker, D.; Zilliox, J. G. *J. Chim. Phys.* **1966**, *63*, 1507−1514.
(26) Beuermann, S.; Paquet, D. A., Jr.; McMinn, J. H.; Hutchinson, R. A. *Macromolecules* **1996**, *29*, 4206−4215.
(27) Hutchinson, R. A.; McMinn, J. H.; Paquet, D. A., Jr.; Beuermann, S.; Jackson, C. *Ind. Eng. Chem. Res.* **1997**, *36*, 1103−1113.
(28) Beuermann, S.; Buback, M.; Davis, T. P.; Gilbert, R. G.; Hutchinson, R. A.; Olaj, O. F.; Russell, G. T.; Schweer, J.; van Herk, A. M. *Macromol. Chem. Phys.* **1997**, *198*, 1545−1560.
(29) Tulig, T. J; Tirrell, M. *Macromolecules* **1982**, *15*, 459−463.
(30) Brandrup, J., Immergut, E. H., Grulke, E. A., Eds.; *Polymer Handbook*, 4th ed.; Wiley-Interscience: New York, 2003.
(31) Clay, P. A.; Gilbert, R. G. *Macromolecules* **1995**, *28*, 552−569.
(32) Tobita, H.; Shiozaki, H. *Macromol. Theory Simul.* **2001**, *10*, 676−685.
(33) Kukulj, D.; Davis, T. P.; Gilbert, R. G. *Macromolecules* **1998**, *31*, 994−999.
(34) van Berkel, K. Y.; Russell, G. T.; Gilbert, R. G. *Macromolecules* **2005**, *38*, 3214−3224.

MA070908A